The combi-targeting concept: evidence for the formation of a novel inhibitor *in vivo*

Nuria Merayo[a], Zakaria Rachid[a], Qiyu Qiu[a], Fouad Brahimi[a] and Bertrand J. Jean-Claude[a]

With the purpose of developing drugs that can block multiple targets in tumor cells, molecules termed combi-molecules or TZ–I have been designed to be hydrolyzed *in vitro* to TZ + I, where TZ is a DNA-damaging species and I is an inhibitor of the epidermal growth factor receptor (EGFR). Using HPLC and liquid chromatography–mass spectrometry (LC–MS), we investigated the mechanism of *in vivo* degradation of a prototype of one such combi-molecule, ZRBA1, which when administered i.p. rapidly degraded into FD105 (C_{max} = 50 μmol/l, after 30 min), a 6-aminoquinazoline that was *N*-acetylated to give FD105Ac (IAc) (C_{max} = 18 μmol/l, after 4 h). A similar rate of acetylation was observed when independently synthesized FD105 was administered i.p. More importantly, the EGFR binding affinity of IAc was 3-fold greater than that of I, indicating that the latter is converted *in vivo* into an even more potent EGFR inhibitor. The results *in toto* suggest that while *in vitro* TZ–I is only hydrolyzed to I + TZ, further acetylation of I *in vivo* leads to a third component – a highly potent EGFR inhibitor with a delayed C_{max}. *Anti-Cancer Drugs* 17:165–171 © 2006 Lippincott Williams & Wilkins.

Anti-Cancer Drugs 2006, **17**:165–171

Keywords: combi-molecule, epidermal growth factor receptor inhibitor, pharmacokinetics, triazene

[a]Cancer Drug Research Laboratory, Department of Medicine, McGill University Health Center, Royal Victoria Hospital, Montreal, Quebec, Canada.

Correspondence to B.J. Jean-Claude, Cancer Drug Research Laboratory, Department of Medicine, McGill University Health Center, 687 Pine Avenue West, Royal Victoria Hospital, Rm M7 19, Montreal, Quebec H3A 1A1, Canada. Tel: +1 514 934-1934; fax: +1 514 843-1475; e-mail: bertrandj.jean-claude@mcgill.ca

Received 23 September 2005 **Accepted** 23 September 2005

Introduction

Refractory tumors are characterized by a variety of dysfunctions including overexpression and dysregulation of many receptor tyrosine kinases (TKs). One such receptor, epidermal growth factor receptor (EGFR), is often overexpressed in breast, ovarian and prostate tumors [1–7], and this can result in the formation of autocrine loops associated with aggressive tumor growth and poor patient prognosis [1,7–9]. Blocking EGFR-mediated signaling has already been shown to induce anti-tumor activity *in vivo* [2,10–14]. However, most EGFR inhibitors induce reversible activity and in many cases blocking a single target does not suffice to eradicate the tumor. To circumvent this problem, we recently designed a novel strategy termed 'combi-targeting' that seeks to synthesize molecules referred to as combi-molecules or TZ–I, designed to not only block EGFR on their own (Fig. 1), but also induce cell killing by damaging DNA [15–23]. As outlined in Fig. 1(a), these molecules were also designed to generate an additional EGFR inhibitor I following hydrolytic cleavage. Thus, we postulated that the combi-molecule, being an agent with multiple effects, should induce more potent anti-proliferative activity than classical alkylators and the current EGFR inhibitors alone. We have now verified these postulates using various TZ–Is of the triazenoquinazoline class and degradation studies *in vitro* clearly demonstrated the formation of 6-aminoquinazolines (I) following hydrolytic cleavage of the 1,2,3-triazene chain [17,19,21]. The formation of the metastable alkylating diazonium species (TZ) has already been demonstrated by radiotracing [17].

Recently, we developed a novel TZ–I termed ZRBA1 that showed significant activity *in vivo* against the human breast cancer xenograft MDA-MB468 administered i.p. [24] and *in vitro* degradation study demonstrated that it was slowly hydrolyzed to FD105 (I) in cell culture medium (Fig. 2). Thus, it was proposed that ZRBA1, while capable of blocking EGFR TK (see TZ–I-EGFR) on its own, can degrade into FD105 (I) that further blocks EGFR TK (see I-EGFR) plus dimethylethyldiazonium (TZ) that damages DNA through its aziridinium intermediate (TZ-DNA). The formation of FD105 from the degradation of ZRBA1 has now been demonstrated and that of the alkylating species indirectly confirmed by the significant levels of DNA strand breaks that it induced *in vitro* [24]. While the rate of conversion of ZRBA1 into FD105 has now been determined, the exact nature of the released alkylating moiety (TZ) remained unknown. Thus, this has stimulated our interest in characterizing the alkylating species using *p*-nitrobenzylpyridine (NBP) [25] and mass spectrometry (MS). We also studied its fate following i.p. injection – a route of

0959-4973

administration by which it demonstrated significant potency in xenograft models [24]. Here, we studied (i) the superior potency of ZRBA1 when compared with a two-drug combination involving the clinical triazene temozolomide + FD105 in an anti-proliferative assay *in vitro*, (ii) the kinetics of absorption/elimination of ZRBA1, and (iii) its *in vivo* metabolism by LC-MS analyses.

Materials and methods

HPLC and LC-MS analyses

HPLC was performed using a Thermoquest (Mississauga, Canada) P4000 with a UV3000 detector and AS300 autosampler. Mass spectra were obtained with a Finnigan (Montreal, Canada) LC QDUO spectrometer.

Fig. 1

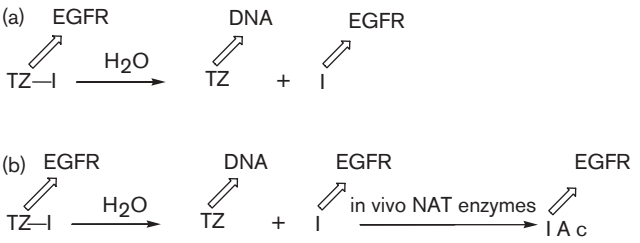

General equation for the hydrolysis of the combi-molecule TZ-I *in vitro* and *in vivo*.

Chemicals

HPLC-grade solvents were purchased from Produits Chimiques ACP (Montreal, Quebec, Canada). FD105 and ZRBA1 were synthesized according to a previous published procedure [19]. Independent synthesis of FD105Ac was performed according to the procedure described herein.

Synthesis of ZRBA1

The 6-amino-4-[(3-chlorophenyl)amino]quinazoline [19] **1** (500 mg, 1.70 mmol). was stirred in dry acetonitrile (15 ml) under argon, after which the solution was cooled to −5°C followed by the addition of nitrosonium tetrafluoroborate (430 mg, 3.70 mmol) in acetonitrile. The resulting clear solution was stirred for 1 h at −5°C to permit the formation of the diazonium salt. It was then added dropwise to another solution of ether (20 ml), water (3 ml), Et_3N (1 ml) and *N,N*-dimethylethylenediamine (1.50 ml, 11.90 mmol) at 0°C. The mixture was stirred at room temperature overnight followed by subsequent extraction with ethyl acetate. The organic layer was dried over potassium carbonate and evaporated to provide the crude product which was purified by chromatography using a basic alumina column (1:3 triethylamine-AcOEt) to give an oil that solidified upon addition of petroleum ether and ether to give (200 mg, 29%) ZRBA1; m.p. 150°C; ^{1}H-NMR (400 MHz, DMSO-d_6) δ 10.63 (br, s, 1H, N = N-NH), 9.89 (s, 1H, NH), 8.57 (s, 1H, H-5), 8.41 (s, 1H, H-2), 8.14 (s, 1H, H-2′), 7.94 (d, 1H, J = 8.8 Hz, H-7), 7.87 (d, 1H, J = 8.8 Hz, H-8), 7.75 (d, 1H, J = 9.5 Hz, H-4′), 7.38 (t, 1H, J = 9.5 Hz,

Fig. 2

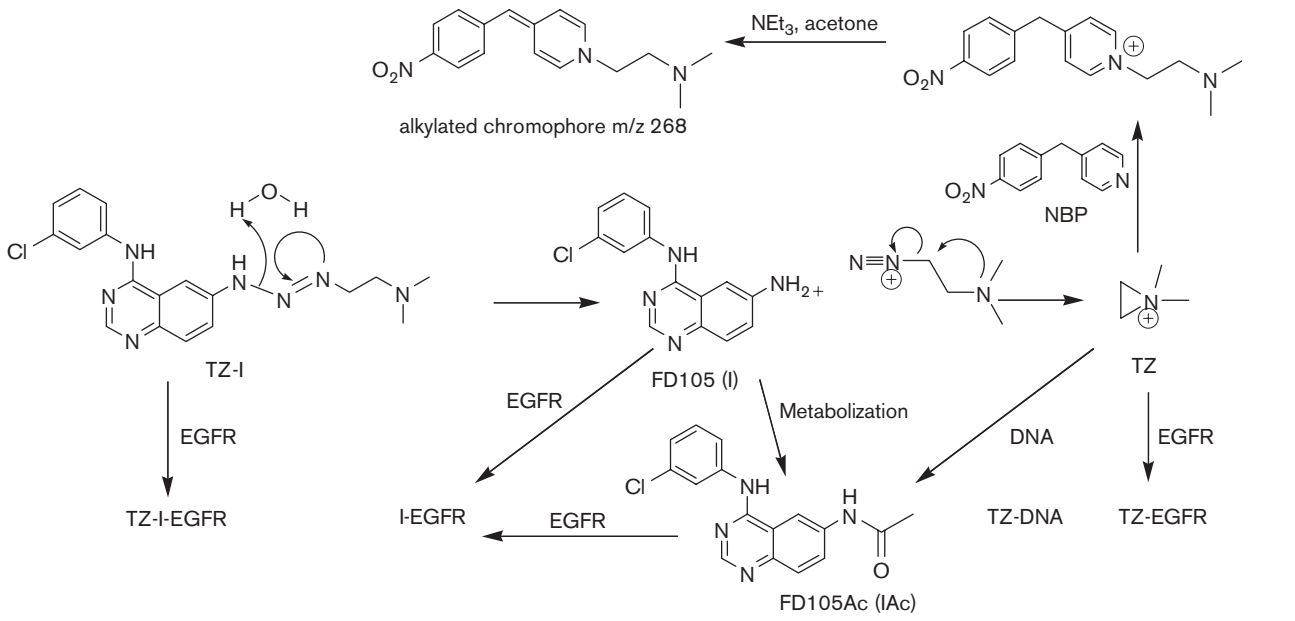

Mechanism of decomposition of the TZ-I ZRBA1 and alkylation of NBP of DNA by the released active species.

H-5′), 7.13 (d, 1H, $J = 9.5$ Hz, H-6′), 3.66 (br, q, 2H, CH_2), 2.56 (t, 2H, $J = 8.6$ Hz, CH_2), 2.19 (s, 6H, $2 \times CH_3$); ^{13}C-NMR (100 MHz, DMSO-d_6) d 157.1, 152.8, 148.8, 147.8, 141.0, 130.1, 128.6, 125.5, 124.6, 123.8, 121.0, 120.3, 115.5, 114.4, 55.3, 45.2 (2C overlap), 41.5.

Synthesis of FD105Ac

Acetic anhydride (0.12 ml). was added to a solution of FD105 [19] (50 mg, 0.185 mmol) in acetic acid (0.3 ml). After 4 h, NaOH (2.3 ml, 10%) was added. The light brown precipitate that formed was filtered, washed with ethanol and recrystallized from dichloromethane (40 mg, 70%). ^{1}H-NMR (300 MHz, DMSO-d_6) δ 2.13(s, CH_3), 7.16 (ddd, 1H, $J = 0.9$, 2.1, 8.0 Hz, H-6′), 7.40 (dd, 1H, $J = 8.1$, 8.0 Hz, H-5′), 7.73-7.78 (m, 2H, H-7, H-4′), 7.85 (dd, 1H, $J = 2.1$, 8.1 Hz, H-8), 7.99 (br, s, 1H, H-2′), 8.57 (s, 1H, H-2), 8.67 (d, 1H, $J = 1.8$ Hz, H-5), 10.05 (br, s, 1H, NH), 10.35 (s, 1H, NH); ^{13}C-NMR (100 MHz, DMSO-d_6) δ 24.7, 112.5, 116.2, 120.7, 121.7, 123.3, 127.2, 128.8, 130.6, 133.3, 141.9, 145.2, 146.8, 153.4, 157.9, 169.2.

Cell culture

DU145 cells (ATCC, Manassas, Virginia, USA) were maintained in RPMI 1640 supplemented with FBS (10%) and ciprofloxacin 10 μg/ml (Mediatech, Herndon, Virginia, USA). The cultures were kept in logarithmic growth by harvesting with a trypsin–EDTA solution containing 0.5 mg/ml trypsin and 0.2 mg/ml EDTA, and replating before confluence. All cell lines used herein were repeatedly tested negative for mycoplasma contaminations.

Growth inhibition studies

Cell monolayers were exposed to different concentrations of each compound continuously for 120 h or, for the FD105 + TEM combination, the drugs were mixed at a 1:7 molar ratio, serially diluted and added to the monolayers for 120 h. The nature of drug interactions was determined using:

$$CI_{50} = [IC_{50}(\text{TEM in combination})/IC_{50}(\text{TEM alone})] + [IC_{50}(\text{FD105 in combination})/IC_{50} \times (\text{FD105 alone})] \quad (1)$$

where $CI_{50} > 1$, $CI_{50} = 1$ or $CI_{50} < 1$ would indicate, antagonism, additivity or synergism, respectively.

All growth inhibitory activities were evaluated using the SRB assay [26]. Briefly, cells were fixed using 50 μl of cold TCA (50%) for 60 min at 4°C, washed five times with tap water and stained for 30 min at room temperature with SRB (0.4%) dissolved in acetic acid (1%). The plates were rinsed five times with 1% acetic acid and allowed to air dry. The resulting colored residue was dissolved in 200 μl of Tris base (10 mmol/l) and optical density was read for each well at 540 nm using a Bio-Rad (Hercules, California, USA) microplate reader (model 2550). Each point represents the average of at least two independent experiments run in triplicate and IC_{50} values were calculated with the GraphPad Prism software package.

Pharmacokinetics

All studies were performed in CD-1 male mice (20–22 g) using two or three animals per time point. The drug was administered i.p. at 100 mg/kg in 0.4 ml of a Tween 80 (6%)/ethanol (6%) saline solution. At each time point, blood samples were collected in heparinized tubes, centrifuged for 8 min at 3000 r.p.m., and the supernatant (plasma) separated with a micropipette and stored at –80°C. The standard samples were prepared by mixing 1 μl of the desired DMSO solution of ZRBA1, FD105 or its metabolite with 24 μl of plasma. The mixture was extracted with acetonitrile, centrifuged for 5 min at 3000 r.p.m. and the supernatant analyzed by HPLC.

Sample preparation

Plasma aliquots (50 μl) were mixed with methanol (100 μl) to precipitate the proteins and the mixture centrifuged for 5 min at 6000 r.p.m. An aliquot was filtered and measured by HPLC.

HPLC method

A C_{18} column ChromBa (4 × 300 mm, 10 μm particle size) was used with methanol:water (7:3) (pH 8, reached with KOH) as mobile phase at 0.8 ml/min. and 20 μl of the supernatant was injected at each time point.

Kinase assay

The EGFR kinase assay is similar to the one described previously [27]. Nunc (Roskilde, Denmark) Maxisorp 96-well plates were incubated overnight at 37°C with 0.25 mg/ml poly(L-glutamic acid:L-tyrosine, 4:1) (PGT) in PBS. The kinase reaction was performed by using 4.5 ng/well EGFR affinity purified from A431 cells. The compound was added and phosphorylation initiated by the addition of ATP (50 μmol/l). After 8 min at room temperature, the reaction was terminated by aspiration of the reaction mixture and phosphorylated PGT was detected with horseradish peroxidase-conjugated PY20 anti-phosphotyrosine antibody (Santa Cruz Biotechnology, Santa Cruz, California, USA). The signals were developed by the addition of 3,3′,5,5′-tetramethylbenzidine peroxidase substrate and H_2SO_4 (0.09 mol/l) was added to stop the reaction. The plates were read at 450 nm using a Bio-Rad ELISA reader (model 2550).

Alkylating activity assay

ZRBA1 (10 μl) from a 100 mmol/l stock solution was added to a 2% NBP:ethylene glycol solution (100 μl), mixed with Tris, pH 7.5. (27% ethanol) (70 μl) and incubated at 37°C for 4 h. The color was developed with a

Fig. 3

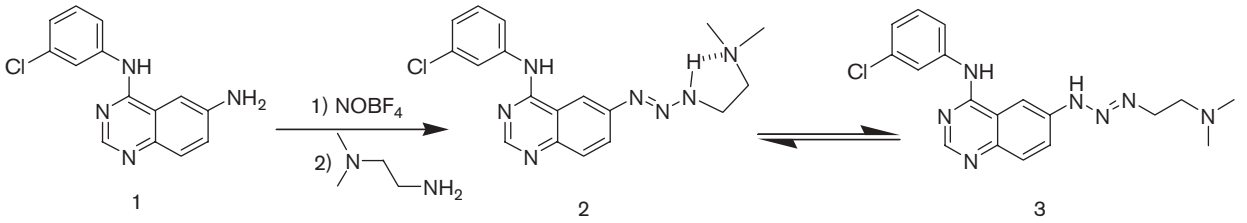

Synthesis of ZRBA1 (2) and its tautomeric equilibrium with 3.

Fig. 4

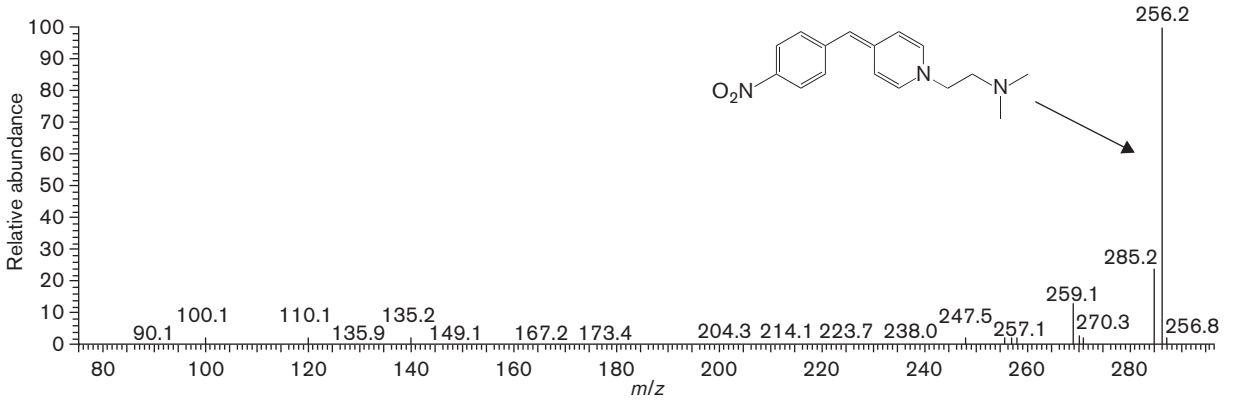

MS data for the identification of the alkylated product obtained from the NBP trapping of the alkylating species released from ZRBA1.

solution of acetone:triethylamine (50/50, v/v) and the resulting mixture analyzed by MS.

Results

Chemistry of ZBRA1

The synthesis of ZRBA1 proceeded according to Fig. 3 by treating aminoquinazoline **1** with nitrosonium tetrafluoborate and coupling the resulting diazonium *in situ* with dimethylethylamine to give the desired triazene **2** (Fig. 3). In solution, triazenes of the ZRBA1 class exist as a mixture of tautomers as shown in Fig. 2 and the higher the proportion of non-conjugated tautomer of type **3**, the least stable they are [28–31]. This is due to rapid decomposition of the latter form through loss of N_2 or hydrolytic cleavage of the triazene chain. In ZRBA1, the conjugated tautomer is expected to be the more abundant as it can be stabilized by intramolecular hydrogen bonding as depicted in Fig. 3. This is further corroborated by NMR spectroscopy that showed a quadruplet at 3.66 p.p.m., confirming the presence of the CH_2NH moiety that characterized the conjugated tautomer **2**.

NBP trapping

In order to identify the TZ release from ZRBA1, we allowed it to react with NBP at physiological pH and temperature for 4 h, and the resulting solution was characterized by MS. A peak at $m/z = 286$ $(M–H)^+$ allowed us to propose the structure of the chromophore (Fig. 2). The mass addition of 72 corresponds to that of the dimethylaminoethyl moiety of TZ, confirming that the latter is indeed released from ZRBA1 (Fig. 4).

In-vitro potency

Prior to embarking on in-vivo pharmacokinetics, we determined whether the activity of ZRBA1 as a combi-molecule was superior to a two-drug combination involving FD105 and temozolomide which releases methyldiazonium *in vivo* [32]. Using the SRB assay in DU145 cells, it was found that the combination of FD105 + temozolomide was subadditive and, more importantly, the anti-proliferative potency of ZRBA1 was approximately 7-fold superior to that of a two-drug combination. Thus, the study of the degradation of the combi-molecule was further carried out *in vivo*.

Fig. 5

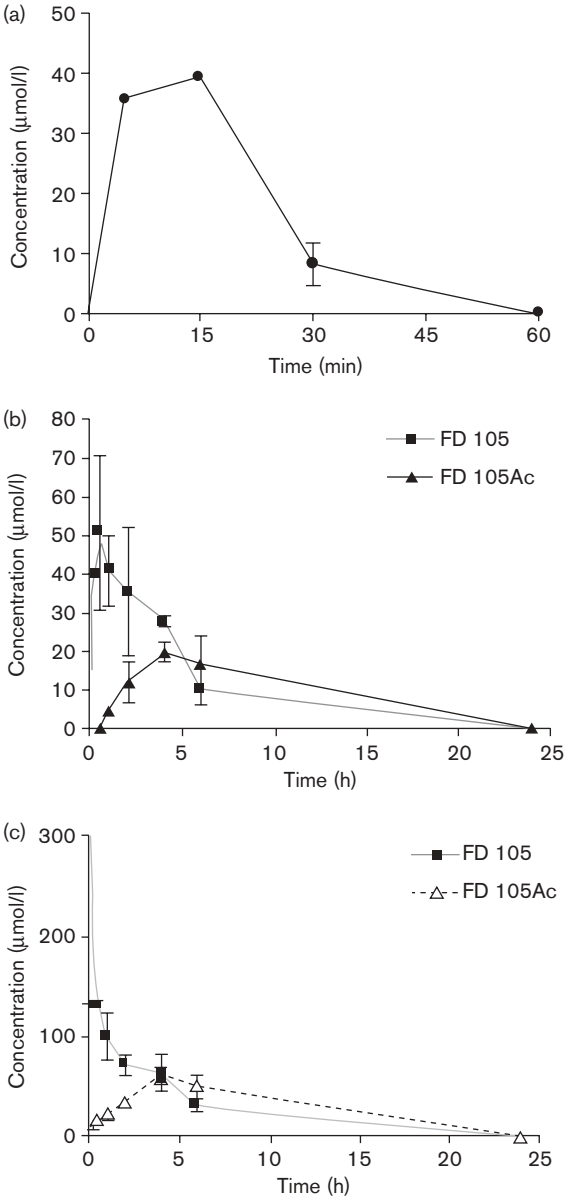

Concentration–time profiles for (a) ZRBA1 given i.p., (b) FD105 and FD105Ac released from ZRBA1, and (c) FD105Ac released from direct administration of FD105.

Fig. 6

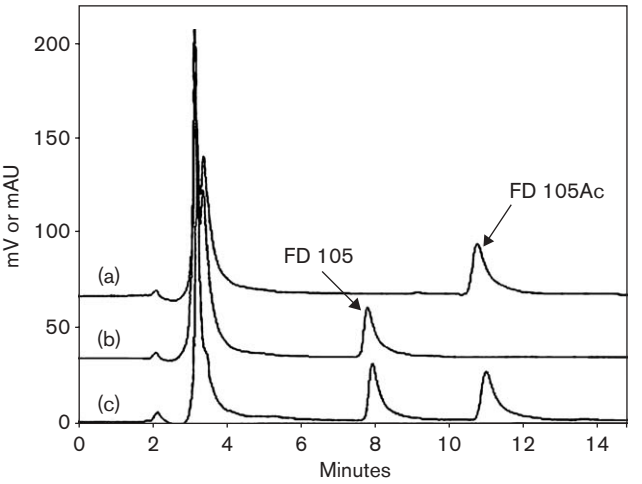

HPLC chromatograms obtained from analyses of (a) pure FD105Ac dissolved in mouse plasma, (b) pure FD105 redissolved in mouse plasma and (c) plasma isolated from mice 4 h after FD105 injection.

In-vivo degradation

Previous work demonstrated that in aqueous media ZRBA1 was slowly converted to the aminoquinazoline FD105 and an alkylating species ($t_{1/2} = 90$ min). However, its degradation profile *in vivo* remained largely unknown. Thus, we characterized the metabolites released in plasma following i.p. administration in CD-1 male mice. Interestingly, significant levels of ZRBA1 were detected in plasma 15 min after its i.p. administration ($C_{max} = 40$ μmol/l) (Fig. 5a), at which time FD105 started being observed. Further characterization of chromatograms obtained from plasma using LC-MS revealed the appearance of a new peak 1 h after administration (Fig. 5b). LC-MS analysis showed a molecular ion at 313 corresponding to the *N*-acetylated product of FD105. Independent synthesis of the putative structure confirmed that this metabolite was indeed 6-*N*-acetyl-(3′-chloroanilino)quinazoline (FD105Ac). Further analysis showed accurate peak matching between chromatograms associated with a standard sample and the product extracted from plasma (Fig. 6).

In order to ascertain the origin of the FD105Ac, FD105 was administered directly i.p. and the resulting metabolite analyzed. FD105 reached its maximum peak plasma level ($C_{max} = 240$ μmol/l) after 15 min (Fig. 5c) and, as in ZRBA1-injected mice, significant levels of FD105Ac were observed. Interestingly, the ratio C_{max}FD105/C_{max}FD105Ac observed following ZRBA1 injection (2.8) was almost identical to that detected from FD105 direct injection (2.7) ($C_{max} = 52$ μmol/l) (Fig. 5c).

In-vitro binding to EGFR

Competitive binding (ELISA) to EGFR was performed to determine inhibitory potency of the new metabolite. As shown in Fig. 7, FD105Ac ($IC_{50} = 0.061$ μmol/l) is three times more potent than FD105 (IC50 = 0.195 μmol/l).

Discussion

A significant number of studies demonstrated that combi-molecules (TZ–I) of the triazene class are hydrolyzed to an aromatic amine (I) and a DNA-damaging species (TZ)

Fig. 7

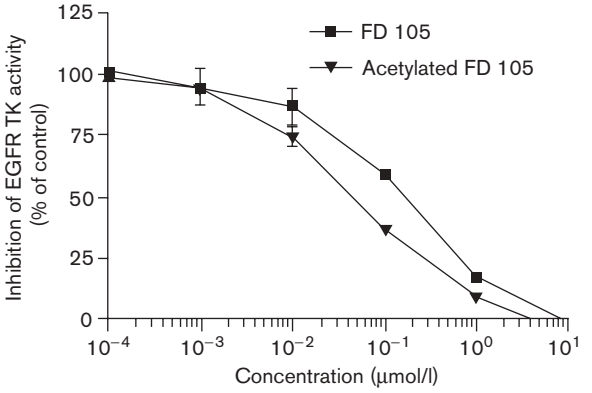

Competitive binding (ELISA) to EGFR by FD105 and acetylated FD105 (FD105Ac). PGT substrate phosphorylation was detected using an anti-phosphotyrosine antibody. Each point represents at least two independent experiments.

leading to equation (1) (Fig. 1) [15–24]. Here, we demonstrated that indeed this translates into 7-fold superior activity when compare to the two-drug combination. The activity of combi-molecules *in vitro* was believed to be a sum of the effects of the intact combi-molecule plus that of the inhibitor I plus the DNA-alkylating species [15,17]. The importance of the released inhibitor I was supported by washout experiments that demonstrated significant loss of anti-proliferative activity when the drug was removed after 2 h cell exposure [23,24]. Since pulse exposure experiments are a good mimic of *in-vivo* absorption, it was feared that the activity of ZRBA1 would be mitigated by the rapid clearance of the released inhibitor FD105 (I). In contrast, the combi-molecule was found extremely potent in xenograft models [24]. Thus, this stimulated our interest in further determining the fate of the combi-molecule *in vivo* and, more specifically, that of the released metabolite. Interestingly, the results shown herein demonstrated that the released FD105 was further converted into an *N*-acetylated metabolite (FD105Ac) with a much slower clearance and a greater EGFR-inhibitory activity than the combi-molecule and its corresponding I. Thus, the current results suggest that after the rapid clearance of ZRBA1, depletion of EGFR will be maintained through the sequential release of two potent inhibitors FD105 ($IC_{50} = 0.195$ μmol/l, C_{max} attained at 15 min) and FD105Ac ($IC_{50} = 0.061$ μmol/l, C_{max} at 4 h) in the plasma. The acetylation of FD105 may be related to the *N*-acetyltransferase enzymes NAT1 and NAT2, which are known to *N*-acetylate aromatic amines *in vivo* [33–36].

In many tumor cells, it has already been shown that EGF stimulation induces expression of DNA repair enzymes such as XRCC1 and ERCC1, and blockade of EGFR TK activity sensitized them to DNA lesions [37]. Hence, in order to exert significant cytotoxic effects through DNA damage, the combi-molecule must be able to concomitantly induce sustained inhibition of EGFR TK. In this context, the hydrolysis of ZRBA1 to give FD105, which in turn is metabolized into an even more potent EGFR inhibitor *in vivo* with a delayed C_{max}, is a highly significant result and this may play a significant role in the efficacy of the combi-molecular strategy.

References

1 Modjtahedi H, Dean C. The receptor for EGF and its ligands: expression, prognostic value and target for therapy in cancer. *Int J Oncol* 1994; **4**:277–296.
2 Xie H, Turner T, Wang MH, Singh RK, Siegal GP, Wells A. *In vitro* invasiveness of DU-145 human prostate carcinoma cells is modulated by EGF receptor-mediated signals. *Clin Exp Metastasis* 1995; **13**:407–419.
3 Gordon AW, Pegues JC, Johnson GR, Kannan B, Auersperg N, Stromberg K. mRNA phenotyping of the major ligands and receptors of the EGF supergene family in human ovarian epithelial cells. *Cancer Lett* 1995; **89**:63–71.
4 Bast RCJ, Pusztai L, Kerns BJ, MacDonald JA, Jordan P, Daly L, *et al.* Coexpression of the HER-2 gene product, p185HER-2, and epidermal growth factor receptor, p170EGF-R, on epithelial ovarian cancers and normal tissues. *Hybridoma* 1998; **17**:313–321.
5 Scoccia B, Lee YM, Niederberger C, Ilekis JV. Expression of the ErbB family of receptors in ovarian cancer. *J Soc Gynecol Invest* 1998; **5**:161–165.
6 Lamharzi N, Halmos G, Armatis P, Schally AV. Expression of mRNA for luteinizing hormone-releasing receptors and epidermal growth factor receptors in human cancer cell lines. *Int J Oncol* 1998; **12**:671–675.
7 Meden H, Kuhn W. Overexpression of the oncogene c-erbB-2 (HER2, neu) in ovarian cancer: a new prognostic factor. *Eur J Obstet Gynecol Reprod Biol* 1997; **71**:173–179.
8 Chen X, Yeung TK, Wang Z. Enhanced drug resistance in cells coexpressing ErbB2 with EGF receptor or ErbB3. *Biochem Biophys Res Commun* 2000; **277**:757–763.
9 Simpson BJ, Bartlett JM, Macleod KG, Rabiasz G, Miller EP, Rae AL, *et al.* Inhibition of transforming growth factor alpha (TGF-alpha)-mediated growth effects in ovarian cancer cell lines by a tyrosine kinase inhibitor ZM 252868. *Br J Cancer* 1999; **79**:1098–1103.
10 Yaish PA, Gazit P, Gilon C, Levitski A. Blocking of EGF-dependent cell proliferation by EGF receptor kinase inhibitors. *Science* 1988; **242**:933–935.
11 Baselga J. New therapeutic agents targeting the epidermal growth factor receptor. *J Clin Oncol* 2000; **18**:54S–59S.
12 Ciardiello F, Caputo R, Bianco R, Damianco V, Pomatico G, De Placido S, *et al.* Antitumour effect and potentiation of cytotoxic drugs activity in human cancer cells by ZD-1839 (Iressa), an epidermal growth factor receptor-sensitive tyrosine kinase inhibitor. *Clin Cancer Res* 2001; **6**: 2053–2063.
13 Dancey JE, Freidlin B. Targeting epidermal growth factor receptor – are we missing the mark? *Lancet* 2003; **362**:62–64.
14 Lee JY, Park YK, Seo SH, Yang B, Park H, Lee YS. 7-Substituted-[1,4]dioxano[2,3-g]quinazolines as inhibitors of epidermal growth factor receptor kinase. *Arch Pharm Med Chem* 2002; **10**:487–494.
15 Brahimi F, Matheson SL, Dudouit F, McNamee JP, Tari AM, Jean-Claude BJ. Inhibition of epidermal growth factor receptor-mediated signaling by 'Combi-Triazene' BJ2000, a new probe for combi-targeting postulates. *J Pharmacol Exp Ther* 2002; **303**:238–246.
16 Qiu Q, Dudouit F, Matheson SL, Brahimi F, Banerjee R, McNamee JP, *et al.* The combi-targeting concept: a novel 3,3-disubstituted nitrosourea with EGFR tyrosine kinase inhibitory properties. *Cancer Chemother Pharmacol* 2003; **51**:1–10.
17 Matheson SL, McNamee JP, Wang T, Alaoui-Jamali MA, Tari A, Jean-Claude BJ. The Combi-Targeting concept: dissection of the binary mechanism of action of the combi-triazene SMA41 *in vitro* and antiproliferative effects *in vivo*. *J Pharmacol Exp Ther* 2004; **311**:1163–1170.
18 Matheson SL, Mzengeza S, Jean-Claude BJ. Synthesis of 1-[4-(*m*-tolyl)-amino-6-quinazolinyl]-3-[14C]-methyl triazene: a radiolabeled probe for the combi-targeting concept. *J Label Compd Radiopharm* 2003; **46**: 729–735.

19 Rachid Z, Brahimi F, Teoh N, Jean-Claude BJ. The combi-targeting concept: chemical dissection of the dual targeting properties of a series of 'combi-triazenes'. *J Med Chem* 2003; **46**:4313–4321.
20 Qiu Q, Dudouit F, Banerjee R, McNamee JP, Jean-Claude BJ. Inhibition of cell signaling by the combi-nitrosourea FD137 in the androgen independent DU145 prostate cancer cell line. *Prostate* 2004; **59**:13–21.
21 Banerjee R, Rachid Z, Jean-Claude BJ. Synthesis of a prodrug designed to release multiple inhibitors of the epidermal growth factor receptor (EGFR) tyrosine kinase and an alkylating agent: a novel tumour targeting concept. *J Med Chem* 2003; **46**:5546–5551.
22 Matheson SL. *The combi-targeting concept*: a novel tumour targeting strategy [PhD Thesis]. Montreal: McGill University; 2003.
23 Matheson SL, McNamee JP, Jean-Claude BJ. The combi-targeting concept: intracellular fragmentation of the binary epidermal growth factor (EGFR)/DNA-targeting 'combi-triazene' SMA41. *Biochem Pharmacol* 2004; **67**:1131–1138.
24 Brahimi F, Rachid Z, McNamee JP, Alaoui-Jamali MA, Tari AM, Jean-Claude BJ. Mechanism of a novel 'combi-triazene' engineered to possess a polar functional group on the alkylating moiety: evidence for enhancement of potency. *Biochem Pharmacol* 2005; **70**:511–519.
25 Nells HJCF, Alry SC, Sinshelmer JE. Comparison of the alkylation of nicotinamide and 4-(*p*-nitrobenzyl)pyridine for the determination of aliphatic epoxides. *Anal Chem* 1982; **54**:213–216.
26 Skehan P, Storeng R, Scudiero D, Monks A, McMahon J, Vistica D, *et al.* New colorimetric cytotoxicity assay for anti-cancer drug screening. *J Natl Cancer Inst* 1990; **82**:1107–1112.
27 Matheson SL, McNamee J, Jean-Claude BJ. Design of a chimeric 3-methyl-1,2,3-triazene with mixed receptor tyrosine kinase and DNA damaging properties: a novel tumour targeting strategy. *J Pharmacol Exp Ther* 2001; **296**:832–840.
28 LaFrance RJ, Manning HW, Vaughan K. Open-chain nitrogen compounds. Part XII. Methanolysis of 3-alkyl-3,4-dihydro-1,2,3-benzotriazin-4-ols: evidence for ring-chain tautomerism with the cytotoxic monoalkyltriazenes. *Can J Chem* 1987; **65**:292–297.
29 Shealy YF, Krauth CA. Imidazoles. II. 5(or 4)-(Monosubstituted triazeno)imidazole-4(or 5)-carboxamides. *J Med Chem* 1966; **9**: 34–38.
30 Kolar GF, Maurer M, Wildschutte M. 5-(-3-Hydroxymethyl-3-methyl-1-triazeno imidazole-4-carboxamide is a metabolite of 5-(3,3-dimethyl-1-triazeno)-imidazole-4-carboxamide (DIC, DTIC NSC-45388). *Cancer Lett* 1980; **10**: 235–241.
31 Lin AJ, Loo TI. Synthesis and antitumor activity of halogen-substituted 4-(3,3-dimethyl-1-triazeno)quinolines. *J Med Chem* 1978; **21**:268–272.
32 Saleem A, Brown GD, Brady F, Aboagye EO, Osman S, Luthra SK *et al.* Metabolic activation of temozolomide measured *in vivo* using positron emission tomography. *Cancer Res* 2003; **63**: 2409–2415.
33 Meyer UA, Zanger UM. Molecular mechanism of genetic polymorphisms of drug metabolism. *Annu Rev Pharmacol Toxicol* 1997; **37**:269–296.
34 Blum M, Demierre A, Grant DM, Heim M, Meyer UA. Molecular mechanism of slow acetylation of drugs and carcinogens in humans. *Proc Natl Acad Sci USA* 1991; **88**:5237–5241.
35 Boobis AR. Molecular basis for differences in susceptibility to toxicants: introduction. *Toxicol Lett* 1992; **64/65**:109–113.
36 Grant DM, Goodfellow GH, Sugamori KS, Durette K. Pharmacogenetics of the human arylamine *N*-acetyltransferases. *Pharmacology* 2000; **61**: 204–211.
37 Yacoub A, McKinstry R, Hinman D, Chung T, Dent P, Hagan MP. Epidermal growth factor and ionizing radiation up-regulate the DNA repair genes XRCC1 and ERCC1 in DU145 and LNCaP prostate carcinoma through MAPK signaling. *Radiat Res* 2003; **159**:439–452.